

Three-dimensional simulations of the interstellar medium in dwarf galaxies - I. Ram pressure stripping

A. Marcolini¹, F. Brighenti¹ and A. D’Ercole²

¹*Dipartimento di Astronomia, Università di Bologna, via Ranzani 1, 44127 Bologna, Italy*

²*Osservatorio Astronomico di Bologna, via Ranzani 1, 44127 Bologna, Italy*

Accepted ..., Received ...; in original ...

ABSTRACT

We present 3D hydrodynamic simulations of ram pressure stripping in dwarf galaxies. Analogous studies on this subject usually deal with much higher ram pressures, typical of galaxy clusters, or mild ram pressure due to the gas halo of the massive galactic companions. We extend over previous investigations by considering flattened, rotating dwarf galaxies subject to ram pressures typical of poor galaxy groups.

We study the ram pressure effects as a function of several parameters such as galactic mass and velocity, ambient gas density, and angle between the galactic plane and the direction of motion. It turns out that this latter parameter plays a role only when the gas pressure in the galactic centre is comparable to the ram pressure. Despite the low values of the ram pressure, some dwarf galaxies can be completely stripped after 1-2 hundred of million years. This pose an interesting question on the aspect of the descents and, more in general, on the morphological evolution of dwarf galaxies. In cases in which the gas is not completely stripped, the propagation of possible galactic wind may be influenced by the disturbed distribution of the interstellar matter.

We also consider the modification of the ISM surface density induced by the ram pressure and find that the resulting compression may trigger star formation over long time spans.

Key words: galaxies: clusters: general – galaxies: dwarfs – galaxies: kinematics and dynamics – hydrodynamics: numerical.

1 INTRODUCTION

Galaxies are not closed boxes and their evolution is closely connected with episodes of interstellar matter (ISM) losses. These losses are due to internal mechanisms such as galactic winds, or external mechanisms as the ram pressure stripping exerted on a galaxy moving through the external intracluster/intergalactic medium (ICM/IGM).

Since dwarf galaxies have small escape velocities, both galactic winds and ram pressure stripping are expected to be more efficient than for giant galaxies. Dwarf irregulars (dIrrs) often have lower abundances than those predicted by the closed box chemical models (cf. Matteucci & Chiosi 1983). This is generally taken as evidence of metal enhanced outflow via galactic winds, although the same effect can also be achieved by stripping of the gas (Skillman 2001).

The effect of the ram pressure on a dwarf galaxy evolution goes beyond the mere reduction of the ISM mass. In fact, the ram pressure may influence substantially the dynamics of galactic outflows, both in models in which the wind breaks out of the galactic disk (e.g. De Young & Heckman 1994, MacLow & Ferrara 1999, D’Ercole &

Brighenti 1999, Strickland & Stevens 2000) and models in which the wind is suffocated by an hypothesized extended gaseous halo and remains trapped in the neighborhood of the galaxy (Tenorio-Tagle 1996, and Silich & Tenorio-Tagle 2001). Therefore the ram pressure may be an important factor for the galactic chemical enrichment. A detailed study of the ram pressure - galactic wind interaction will be presented elsewhere (Marcolini, Brighenti and D’Ercole, in preparation). In the present paper we focus on the ISM removal by ram pressure, which is an interesting phenomenon on its own.

In fact, besides the interaction with the galactic wind, the ICM ram pressure can be important also in triggering the starburst which gives rise to the wind itself. Numerical simulations carried with the smoothed-particle hydrodynamics (Abadi, Moore and Bower 1999, Shulz & Struck 2001) and with N -body codes (Vollmer et al. 2001) show that, for small inclination angles (nearly edge-on stripping), the ram pressure leads to a temporary increase of the central gas surface density. This, in turn, may give rise to an episode of star formation.

Ram pressure stripping is also advocated to claim the

arXiv:astro-ph/0309026v1 1 Sep 2003

dIrrs and “transition-type dwarfs” as progenitors of the dwarf spheroidal (dSph) galaxies (Grebel, Gallagher and Harbeck 2003). These latter galaxies experienced star formation over extended time spans in their youths, but today they are free of detectable ISM. Being the galactic winds generally unable to remove a large fraction of the galactic gas (Mac-Low & Ferrara 1999; D’Ercole & Brighenti 1999), an external mechanism as ram pressure has been suggested to strip the ISM. The “transition-type dwarfs” have mixed dIrr/dSph morphologies, low stellar masses, low angular momentum, and HI content of at most a few $10^6 M_\odot$. These dwarfs would closely resemble dSphs if their gas were removed, and are thus likely dSph progenitors.

Several papers investigated the gas dynamics of massive spiral galaxies moving through the ICM of rich clusters (cf. Schulz & Struck 2001 and references therein). Few investigations discussed the effect of stripping for dwarf galaxies. Mori & Burkert (2000) and Murakami & Babul (1999) considered spherical dwarf galaxies moving through a dense ICM with velocities $\sim 1000 \text{ km s}^{-1}$, typical of clusters of galaxies. Sofue (1994a,b) studied the moderate stripping on spherical dwarf galaxies due to their motion through the gas halo of larger companions. He adopted an N -body code and investigated the different behaviour of HI and molecular gas, but some genuine hydrodynamic phenomena such as shock waves and Kelvin-Helmholtz (K-H) instabilities are inevitably ignored.

In this work we make use instead of pure hydrodynamical simulations (cf. the discussion at the end of section 6), and study *disky* dwarf galaxies orbiting inside small galaxy groups, where most of these galaxies reside (Nolthenius 1993). Even dwarfs now in clusters have likely spent a significant fraction of their life in loose groups, before enter a cluster as the hierarchical growth of the structures proceeded.

Velocity dispersions in groups are much lower than in rich clusters, and the ram pressure stripping is much reduced. However, even though the low ram pressure in groups is often unable to completely remove the galactic gas, it may be still effective in stripping the outer part of the ISM and affecting the gas distribution inside the galaxy (Bureau and Carignan 2002, Hidaka & Sofue 2002). Moreover, ram pressure due to gaseous halos of the Milky Way and M31 has been advocated by Van den Bergh (1994) to explain the observed correlation between stellar content and galactocentric distance of dwarf galaxies.

To investigate this important evolutionary phase in the life of dwarf galaxies, we have undertaken a systematic study of the interaction between IGM/ICM and the ISM. We run a number of 3D and 2D hydrodynamic simulations in which we varied several parameters, as the galaxy mass, the ram pressure strength, and the inclination between the galaxy and the direction of its motion.

2 THE MODEL

2.1 Potential well

The gravitational potential of our models is due to the contribution of two mass distributions: a spherical quasi-isothermal dark matter halo and a stellar thin disk. The dark matter halo density is given by:

$$\rho_h(r) = \frac{\rho_{0h}}{\left[1 + \left(\frac{r}{r_h}\right)^2\right]}, \quad (1)$$

where ρ_{0h} is the central density and r_h is the core radius. The distance to the centre is given by $r = \sqrt{R^2 + z^2}$, where R is the radius on the equatorial plane ($z = 0$). The dark halo is truncated at a radius r_{tr} , and its mass as a function of $x = r/r_h$ is then:

$$M_h(r) = 4\pi\rho_{0h}r_h^3(x - \arctan x). \quad (2)$$

With these assumptions the gravitational potential of the halo is given by:

$$\Phi_h(r) = \begin{cases} 4\pi G\rho_{0h}r_h^2\left\{-1 + \frac{\arctan x}{x} + \frac{1}{2}[\log(1+x^2) - \log(1+\psi^2)]\right\}, & r \leq r_{tr} \\ -\frac{GM_{h,tot}}{r}, & r > r_{tr} \end{cases} \quad (3)$$

where $\psi = r_{tr}/r_h$ and $M_{h,tot} = M_h(r_{tr})$.

We assume that the stars are distributed in an infinitesimally thin Kuzmin’s disk with surface density (cf. Binney & Tremaine 1987):

$$\Sigma_*(R) = \frac{aM_*}{2\pi(R^2 + a^2)^{3/2}}, \quad (4)$$

where M_* is the total mass of stars and a is a radial scale-length. The stellar potential generated by this mass distribution is:

$$\Phi_*(R, z) = -\frac{GM_*}{\sqrt{R^2 + (a + |z|)^2}}. \quad (5)$$

We consider three different galactic models differing mainly for their masses and hereafter called small (SM), intermediate (MD) and large (LG) (see Table 1).

2.2 Gas distribution

The ISM is assumed to be single-phase, isothermal and in rotational equilibrium with the potential Φ generated by the dark matter halo plus the stellar thin disk.

To obtain a realistic profile of the rotation curve and the surface density we proceed as follow (cfr. D’Ercole & Brighenti 1999). First we assume a gas distribution in the equatorial plane ($z = 0$) of the form:

$$\rho(R, 0) = \frac{\rho_0}{\left(1 + \left(\frac{R}{R_c}\right)^2\right)^2}. \quad (6)$$

Then, in order to build a rotating ISM configuration in equilibrium with the given potential Φ , we solve the steady state momentum equation:

$$(v \cdot \nabla)v = -\frac{1}{\rho}\nabla(P) - \nabla\Phi. \quad (7)$$

The rotational velocity in the equatorial plane is given by the equilibrium condition:

$$v_\phi^2(R, 0) = v_{\text{cir}}^2 - \frac{R}{\rho} \left| \frac{dP}{dR} \right|_{z=0}, \quad (8)$$

where $v_{\text{cir}} = \sqrt{R\partial\Phi/\partial R}$ is the circular velocity and P the thermal gas pressure. The gas distribution out of the plane is obtained integrating the z component of the hydrostatic equilibrium equation for any R . The resulting gaseous disk shows a pronounced flare (see upper panels *a* in Fig. 4, discussed below), a consequence of the assumption that v_ϕ does

not depend on z . This assumption is necessary to have an isothermal gas in rotational equilibrium (Tassoul 1978). We stress that the basic results of our simulations do not depend on the presence of this (somewhat unrealistic) flare. With an appropriate choice of the parameters ρ_0 and R_c (Table 2) we obtain realistic radial profiles of the column densities and circular velocities (Swaters 1999) for our three models, as shown in Fig. 1 and 2.

In the following, we shall investigate the variation of the mass of gas, induced by the ram pressure stripping, in two regions: the *galactic region* and the *central region*. The first is intended to contain the “total” amount of ISM M_{gal} associated to the galaxy. It is defined as a cylindrical volume within $z < |z_{\text{gal}}|$ and $R < R_{\text{gal}}$, where the values of $|z_{\text{gal}}|$ and R_{gal} for the various models are given in Table 2. The second, smaller region roughly represents the volume of the stellar disk of the galaxy and provides a measurement of the central content of ISM M_{centr} . It is defined by $z < |z_{\text{centr}}|$ and $R < R_{\text{centr}}$, where $|z_{\text{centr}}|$ and R_{centr} are again given in Table 2. We believe that the analysis of gas removal in these two regions is more meaningful and instructive than the simple computation of the ISM in the computational grid, which extends to a very large distance from the galactic centre (section 4). The initial amount of gas in these two regions is given in Table 2.

Finally, we considered also a non rotating galaxy (model NR) having exactly the same potential well of the MD model, but in which the ISM does not rotate. This model was run to consider the effect of the presence of a spheroidal gaseous halo around the galaxy. Such a halo is important also in view of its influence on the evolution of the possible galactic wind. In order to obtain an halo extension comparable to the galactic size, we adopted an ISM temperature which is somewhat larger than that of the ISM in the MD model, as shown in Table 2. The gas distribution is simply specified by the (isothermal) hydrostatic equilibrium condition, with the central density given in Table 2.

2.3 The ram pressure

We are interested in ram pressure values characteristic for poor galaxy groups. Group velocity dispersions of few hundred km s^{-1} are typical (Zabludoff & Mulchaey 1998). Characteristic IGM densities are $n \sim 10^{-4} - 10^{-3} \text{ cm}^{-3}$ (e.g. Mushotzky et al. 2003). We thus considered for each of our models two values for the ram pressure $P_{\text{ram}} = \rho_{\text{IGM}} v_{\text{IGM}}^2$ within the range of typical values: $P_{\text{LOW}} = 8 \times 10^{-14} \text{ dyn cm}^{-2}$ and $P_{\text{HIGH}} = 3.2 \times 10^{-12} \text{ dyn cm}^{-2}$. The first case is realised with the density-velocity combination $(\rho_{\text{IGM}}, v_{\text{IGM}}) = (2 \times 10^{-28} \text{ g cm}^{-3}, 200 \text{ km s}^{-1})$, while the latter with $(\rho_{\text{IGM}}, v_{\text{IGM}}) = (2 \times 10^{-27} \text{ g cm}^{-3}, 400 \text{ km s}^{-1})$. The IGM parameters are summarized in Table 3. The temperature of the IGM is $T_{\text{IGM}} = 10^6 \text{ K}$ for both cases. This temperature is somewhat lower than that predicted by the observed $\sigma - T$ relation for galaxy groups (Helsdon & Ponman 2000), assuming $\sigma \sim v_{\text{IGM}}/\sqrt{3}$. The choice of a low T_{IGM} has been guided by the desire to have galaxies moving supersonically through the IGM. In this regime, any numerical perturbation does not propagate upstream and does not interfere with the “inflow” boundary condition there.

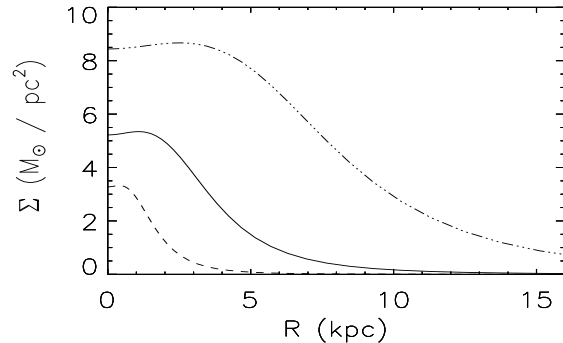


Figure 1. Face-on column density profiles of the initial ISM for the three galaxy models: SM (dashed line), MD (solid line) and LG (dashed dotted line).

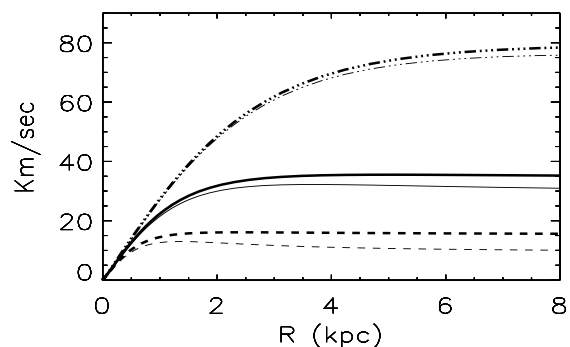


Figure 2. Radial profiles of the circular v_{circ} (thick lines) and rotational v_{ϕ} velocities for the three galaxy models: SM (dashed lines), MD (solid lines) and LG (dashed dotted lines).

3 ANALYTIC CONSIDERATIONS

It is interesting to make some simple prediction about the effectiveness of the ram pressure stripping for both face-on and edge-on models. As discussed by Mori & Burket (2000), the stripping process may be broadly classified into two regimes: the instantaneous stripping and the continuous stripping assisted by Kelvin-Helmholtz (K-H) instabilities.

Instantaneous stripping occurs if the ram pressure is larger than the restoring gravitational force per unit area. In the case of face-on models an analytical estimate of the radius R_{str} beyond which the gas will be stripped is obtained solving the equation (Gunn & Gott 1972):

$$\frac{\partial \Phi}{\partial z}(R_{\text{str}}, z) \sigma_{\text{ISM}}(R_{\text{str}}) = P_{\text{ram}}, \quad (9)$$

where the left-hand side is the restoring force for unit surface. The value of the z component of the gravitational acceleration at any R is chosen to be the maximum along the z direction, and σ_{ISM} is the ISM surface density. In Fig. 3 the restoring force is shown by the continuous curves for the SM, MD and LG galactic models (from the bottom to the top, respectively). The two horizontal lines represent the two values of the ram pressure considered. The intersections

Table 1. Galaxy parameters

| Model | ρ_{0h} (10^{-24} g cm $^{-3}$) | r_h (kpc) | r_{tr} (kpc) | a (kpc) | M_* ($10^8 M_\odot$) | $M_{h,tot}$ ($10^9 M_\odot$) |
|-------|--|----------------|-------------------|--------------|-----------------------------|-----------------------------------|
| SM | 1.4 | 0.45 | 15 | 0.9 | 0.6 | 0.76 |
| MD | 1.4 | 1.00 | 30 | 1.8 | 6.0 | 7.4 |
| LG | 1.4 | 2.30 | 60 | 3.6 | 60.0 | 77.2 |
| NR | 1.4 | 1.00 | 30 | 1.8 | 6.0 | 7.4 |

Table 2. ISM parameters

| Model | ρ_0 (10^{-24} g cm $^{-3}$) | R_c (kpc) | T (10^3 K) | M_{centr} ^(a) ($10^7 M_\odot$) | M_{gal} ^(b) ($10^8 M_\odot$) | R_{centr} (kpc) | $ z_{centr} $ (kpc) | R_{gal} (kpc) | $ z_{gal} $ (kpc) |
|-------|---|------------------|--------------------|--|--|----------------------|------------------------|--------------------|----------------------|
| SM | 1.0 | 1.2 | 2.3 | 0.9 | 0.5 | 1.0 | 0.5 | 4.0 | 1.0 |
| MD | 2.0 | 2.4 | 4.5 | 6.6 | 4.1 | 2.0 | 1.0 | 8.0 | 2.0 |
| LG | 4.0 | 4.8 | 9.0 | 42.2 | 33.1 | 4.0 | 2.0 | 16.0 | 4.0 |
| NR | 2.0 | - ^(c) | 10.0 | 1.3 | 0.17 | 1.0 ^(d) | 1.0 ^(d) | 4.0 ^(d) | 4.0 ^(d) |

^(a) initial mass content of the central region defined as a cylinder with $R < R_{centr}$ and $z < |z_{centr}|$.

^(b) initial mass content in the galactic region defined as a cylinder with $R < R_{gal}$ and $z < |z_{gal}|$.

^(c) no value for R_c is specified for the static ISM of this model

^(d) for the NR model the central and the galactic regions are spheres with the specified radii.

of these straight lines with the curves individuate R_{str} . If the ram pressure value lies above the maximum of a curve, the galaxy is completely stripped. This is similar to say that P_{ram} exceeds the thermal pressure P_0 at the centre of the gravitational potential well.

As pointed out by several authors (e.g. Schulz & Struck 2001, Vollmer et al. 2001), the differences of the ram pressure effects are not simply explained by the projection cosin law in cases where the IGM wind impacts the galactic disk at a significant angle θ to the disk symmetry axis. In the case of edge-on models, we thus followed a different approach and considered the continuous stripping to obtain a condition similar to equation (9). The most effective K-H modes for stripping are those with wavelengths comparable to the galactic radius R (Nulsen 1982). These modes, however, could be suppressed by the gravity g if this is larger than a critical value (Murray et al. 1993):

$$g_{cr} = \frac{2\pi v_{IGM}^2}{\alpha R}, \quad (10)$$

where α is the ratio between the ISM density and the IGM density at distance R . Equation (10) can be written as:

$$\frac{\rho(R_{str})g(R_{str}, 0)R_{str}}{2\pi} = P_{ram}, \quad (11)$$

and we can individuate the radius R_{str} , at which the ram pressure become less effective in removing the ISM, as the “final” radius of the galaxy. The dashed curves in Fig. 3 represent the left-hand side of the above equation for the SM, MD and LG galactic models (from the bottom to the top, respectively). The outer intersection of these curves with the horizontal lines gives the stable radius R_{str} for the galaxy.

Again, if a particular value of the ram pressure lies above the maximum of these curves, no stable radius can be found and eventually the galaxy will be completely stripped after a characteristic time

$$\tau_{str} \equiv M/\dot{M} \sim \frac{R_{gal}\bar{\alpha}}{v_{IGM}}, \quad (12)$$

where \dot{M} is the (maximum) rate of mass loss, derived by momentum conservation considerations (Nulsen 1982), $\bar{\alpha} = \bar{\rho}/\rho_{ICM}$, and $\bar{\rho}$ is the ISM mean density. Note that, contrary to what reported by some author, this time scale (a lower limit) does not coincide with the characteristic growth scale τ_{KH} of the K-H instability, but is longer by a factor $\bar{\alpha}^{1/2}$.

The couples of continuous (face-on galaxies) and dashed (edge-on galaxies) curves referring to each galaxy model have similar maxima; this would indicate that the orientation of the galaxies is rather unimportant for the complete stripping of the galaxy. However, our numerical simulations show instead that the orientation strongly influences the effectiveness of the stripping when $P_{ram} \sim P_0$ (see section 5). Symbols in Fig. 3 represent the values of R_{str} obtained by our numerical simulations discussed below.

We point out that the Reynold number $Re = 2.8(r/\lambda_{IGM})\mathcal{M}_{IGM}$ (Batchelor 1967) for the IGM is rather high. In fact, for $T_{IGM} = 10^6$ K, Mach number $\mathcal{M}_{IGM} \sim 1$ and $\rho_{IGM} = 2 \times 10^{-27}$ (2×10^{-28}) g cm $^{-3}$, the mean free path is $\lambda_{IGM} \sim 3 \times 10^3 T^2 n_{IGM}^{-1} \approx 1$ (10) pc. With a length scale $r = 10$ kpc we get $Re \sim 10^4$ (10^3). These values are much larger than the critical value ~ 30 (Nulsen 1982) at which the transition from laminar to turbulent flows occurs. By contrast, the effective Reynold number in our simulations is (cf. McKee 1988) $Re \approx rv/c\Delta \sim 60$ (with a zone size $\Delta = 0.5$ kpc at $r = 10$ kpc). Thus, our simulated flows are only marginally turbulent, and the effectiveness of the K-H instability to drive the stripping could be questioned. However, as shown by Nulsen (1982), mass stripping rate for marginally laminar flows is comparable, within a factor of two, with that occurring in fully turbulent flows. We thus conclude that the stripping rates we obtain are still realistic.

4 THE NUMERICAL METHOD

To run the set of simulations we used two hydrocodes: the 3D BOH (BOlogna Hydrodynamics) code and ZEUS-2D (Stone

Table 3. IGM parameters

| Model | ρ_{IGM} (10^{-24} g cm $^{-3}$) | v_{IGM} (km s $^{-1}$) | T_{IGM} (K) |
|-------|--|-------------------------------------|-------------------------|
| LO | 2×10^{-4} | 200 | 10^6 |
| HI | 2×10^{-3} | 400 | 10^6 |

& Norman 1992). The 3D BOH code uses an Eulerian, second order upwind scheme (Bedogni & D’Ercole 1986), in which the consistent advection (Norman, Wilson & Barton 1980) is implemented to reduce numerical diffusion. The 3D version of the code has been tested against a set of hydrodynamic problems with very satisfactory results (Marcolini 2002).

For the models with edge-on or 45° stripping we used the BOH code (in Cartesian coordinates), while for most face-on stripping models we used ZEUS-2D (in cylindrical coordinates). As a test, we run few face-on stripping models with both codes. We found that the differences between the two simulations are negligible.

As most previous investigations (e.g. Mori & Burkert 2000; Quilis, Moore & Bower 2000), we neglect radiative cooling. In order to check whether this assumption affects our results, we run a model including radiative losses (see section 5.1.2). No appreciable differences have been found and we conclude that neglecting radiative cooling is a safe assumption.

The 3D Cartesian grid adopts a non-uniform grid spacing. The central zones are $\Delta x = \Delta y = \Delta z = 20$ pc wide, and the zone size increases geometrically, the size ratio between adjacent zones being 1.1. The $z = 0$ plane coincides with the galactic plane, the z -axis is the rotation axis. Each axis extends from -30 to 30 kpc and contains 106 zones (for the edge-on models we considered only the volume $0 \leq z \leq 30$ kpc, with the z -axis subdivided in 54 zones).

Given the symmetry of the simulation for edge-on models, we use reflecting boundary conditions on the equatorial plane ($z = 0$), inflow conditions on the boundary plane from which the IGM enters the grid ($x = -30$ kpc plane), and outflow conditions on the remaining planes. For 45° models, the inflow conditions are enforced both at the $x = -30$ kpc plane and $z = 30$ kpc plane, while outflow conditions hold on the remaining boundary surfaces of the grid. For 2D face-on cylindrical symmetric models, we have reflecting conditions on the z axis, inflow conditions on the boundary plane $z = 30$ kpc, while outflow conditions are applied at the remaining boundaries.

5 RESULTS

We run 18 simulations for the rotating galaxies, varying the galactic mass, the ram pressure strength, and the inclination angle θ between the galactic plane and galactic velocity. We identify a particular model with the notation XX-YY-ZZ, where XX individuates the galaxy size (SM=small, MD=medium, LG=large, cf. tables 1 and 2); YY expresses the angle θ , and takes the values YY=00 for edge-on models, YY=45 for $\theta = 45^\circ$, and YY=90 for face-on models. Finally,

ZZ represents the value of the ram pressure; ZZ=LO for the weak ram pressure, ZZ=HI for the high one (see table 3).

We also run two models for a non-rotating galaxy, one for each value of the ram pressure (models NR-LO and NR-HI). In these simulations the ram pressure hits the galaxy face-on.

Below we describe in some detail the gasdynamics of the models, paying a special attention to the the representative galaxy “MD”, our reference model.

5.1 The reference model

5.1.1 Model MD-00-LO

Here we describe in some detail the hydrodynamic evolution of the intermediate galaxy model moving edge-on and undergoing the action of the lower ram-pressure. In the upper panels in Fig. 4 (upper strip) the density distribution on the $y = 0$ plane is shown at four different times. The lower panels show the density distribution on the equatorial plane at the same times. The IGM enters the grid from the left boundary. The panels at $t = 0$ represent the initial conditions. After $t = 250$ Myr a rather complex structure is formed. The interaction of the IGM with the ISM gives rise to two shocks: one reflected into the IGM and forming the bow shock, and another transmitted forward through the ISM. The bow shock is rather weak given the low Mach number of the galactic motion ($\mathcal{M} = 1.3$). The transmitted shock, initially with a similar Mach number, propagates in a denser medium and is better discernible in the lower panel *b*. At later times, the lower branch of the transmitted shock wraps quite easily around the core of the galaxy on the equatorial plane, because of the anticlockwise rotation of the ISM. Instead, the upper branch remains nearly stationary (lower panel *c*) because is contrasted by the ISM motion. Later on (lower panel *d*) an asymmetric tail forms downstream. The gas distribution on the disk assumes an elliptical shape because of the compression due to the incoming IGM. The same effect is also apparent in the upper panel *d* where the forward lobe of the ISM is compressed and expands vertically, partially “shielding” the rest of the galaxy by the interaction of the IGM.

In the present model both the instantaneous and the continuous stripping are relatively ineffective in removing the ISM. Figure 5 shows the ISM mass content in both the central and galactic regions; in order to avoid the possible contribution of the IGM, only gas with temperature $T < 3 \times 10^5$ K is considered in these plots. This figure shows that about 90% of the gas is retained in the galactic region, while the central region is essentially unaffected. The central portion of the transmitted shock moving along the x axis has a pressure which is of the order of the ram-pressure, much lower than the ISM pressure P_0 in the central region. As the transmitted shock approaches this region, it becomes weaker and weaker and eventually stalls as a sonic perturbation. The instantaneous stripping is thus effective only at the very outskirts of the galaxy.

The continuous stripping in this model is also rather ineffective, being $\tau_{\text{str}} \gg 1$ Gyr. As pointed out in section 3, in our simulations the continuous stripping occurs essentially via numerical viscosity, while for real galaxies the turbulent stripping is more likely. However, the viscous stripping rate

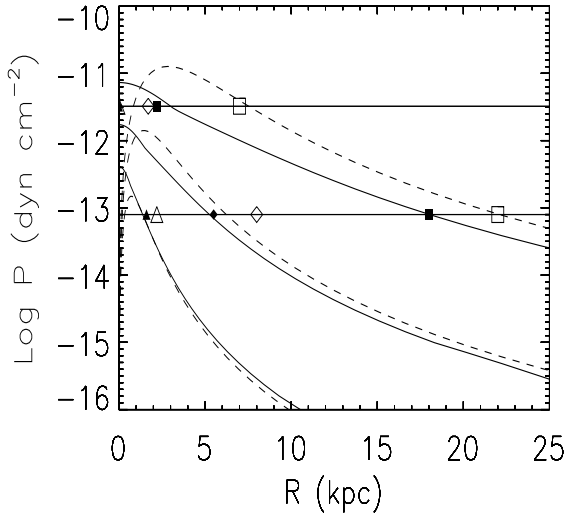


Figure 3. The solid curves represent the radial profile of the maximum value of the z -component of the restoring force for our three galactic models SM, MD and LG (from the bottom to the top, respectively) [equation (9)]. Analogously, the dashed curves represent the gravitational stabilising force of the K-H instabilities [equation (11)]. The horizontal lines represent the lower (LO) and higher (HI) ram pressure values in our models of IGM. The intersections between the solid (dashed) curves and the horizontal lines individuate the final radii in the case of face-on (edge-on) stripping. Symbols represent the radii found in our simulations: triangles, diamonds and squares refer to SM, MD and LG models, respectively. Filled symbols refer to face-on models, while empty symbols refer to edge-on models.

is expected to be comparable with the turbulent stripping (Nulsen 1982). In this latter case the K-H instabilities would be strongly suppressed by the gravity, being $g \gtrsim g_{\text{cr}}$.

5.1.2 Models MD-45-LO and MD-90-LO

The maps of the gas density for model MD-45-LO are shown in the middle strip of Fig. 4. In the upper panels the IGM enters the grid from the left and top boundaries, and crosses the grid diagonally. The external low density lobes are dragged away in a turbulent motion while the ISM in the central region is essentially unaffected. Given the particular direction of the motion, at $t = 100$ Myr two transmitted shocks are present, one in the leading edge of the galaxy and one in the rear of the galaxy (lower panel *b*). At later times, the bow shock is barely visible and the galaxy has a more compact aspect. Also in this case both the galactic and the central regions retain most of its ISM (Fig. 5).

Model MD-90-LO, moving face-on through the IGM, presents a cylindrical symmetry and has been simulated with both the 3D BOH code and with ZEUS-2D. The latter simulation used cylindrical coordinates, with the R -axis and z -axis having the same spacing as the axes of 3D Cartesian grid (see section 4). The two simulations show very similar results, demonstrating the reliability of the two codes. The

model calculated with the 3D code is shown in the lower strip of Fig. 4.

The gas flow keeps a noticeable symmetry up to late times, when the downstream turbulence in the tail of the flow eventually prevails. In the upper panel *b* the transmitted shock is clearly visible as a wing structure. Such a structure is responsible for the ring around the galaxy visible in the lower panel *b*. The galaxy appears truncated on the $z = 0$ plane at the radius $R_{\text{str}} \simeq 5.5$ kpc, in agreement with the value predicted by equation (9) (see also Fig. 3). No ISM is lost from the central region, and only $\sim 20\%$ of gas has been removed from the whole galaxy (Fig. 5).

This model has been run also including radiative cooling. The morphological differences with respect to the adiabatic model are negligible and the stripping rate differs by few percent.

5.1.3 Discussion of model MD-LO

Several galaxies are reported in literature whose distorted and asymmetric HI distributions are claimed to be suggestive of ram pressure stripping by the IGM. Here we consider the dIrr galaxy Holmberg II which has structural parameters similar to those of our model MD (Bureau & Carignan 2002). Actually, the appearance of its ISM (Fig. 3 in the paper of Bureau & Carignan) closely resembles the gas distribution in our model MD-00-LO (lower panel *d* in the upper strip of Fig. 4). This suggests that Holmberg II is moving nearly edge-on through the IGM of the M81 group. Moreover, comparing its asymmetric tail with our simulations, it can be concluded that the galaxy is rotating clockwise on the sky. From a condition similar to equation (9), together with the measurement of the galactic velocity and of the ISM radius, Bureau & Carignan estimate that the value of the IGM density is $n \gtrsim 4 \times 10^{-6} \text{ cm}^{-3}$ at a projected distance of 475 kpc to M81. While equation (9) holds for face-on stripping, our simple analysis shows that the model MD is not sensitive to the value of the inclination angle θ (Fig. 3). Thus, the evaluation of the ICM density given by Bureau & Carignan remains valid.

Numerical simulations confirm that the results of stripping is not very sensitive to θ . Although the effects of the interaction with the IGM in model MD are apparent at large radii, from Fig. 5 it is evident that the gas in the central region is essentially unaffected for any inclination of the galaxy. The amount of ISM in the galactic region is only little more sensitive to the direction of the IGM motion (lower panel *b*). These results are consistent with the analytical predictions given in section 3 and summarised in Fig. 3. The stripping radius of the edge-on model obtained in our numerical simulation results to be a bit larger than that predicted by the Fig. 3. This is due to the long time-scale of the gas ablation, as discussed in section 7.

5.1.4 Models MD-HI

We now briefly describe the same galaxy model of the previous section, in the case of high ram pressure. Contrary to the previous case, now $P_{\text{ram}} = 3.2 \times 10^{-12} \gtrsim P_0 = 1.2 \times 10^{-12} \text{ dyn cm}^{-2}$, and the inclination angle θ becomes a crucial parameter of the problem.

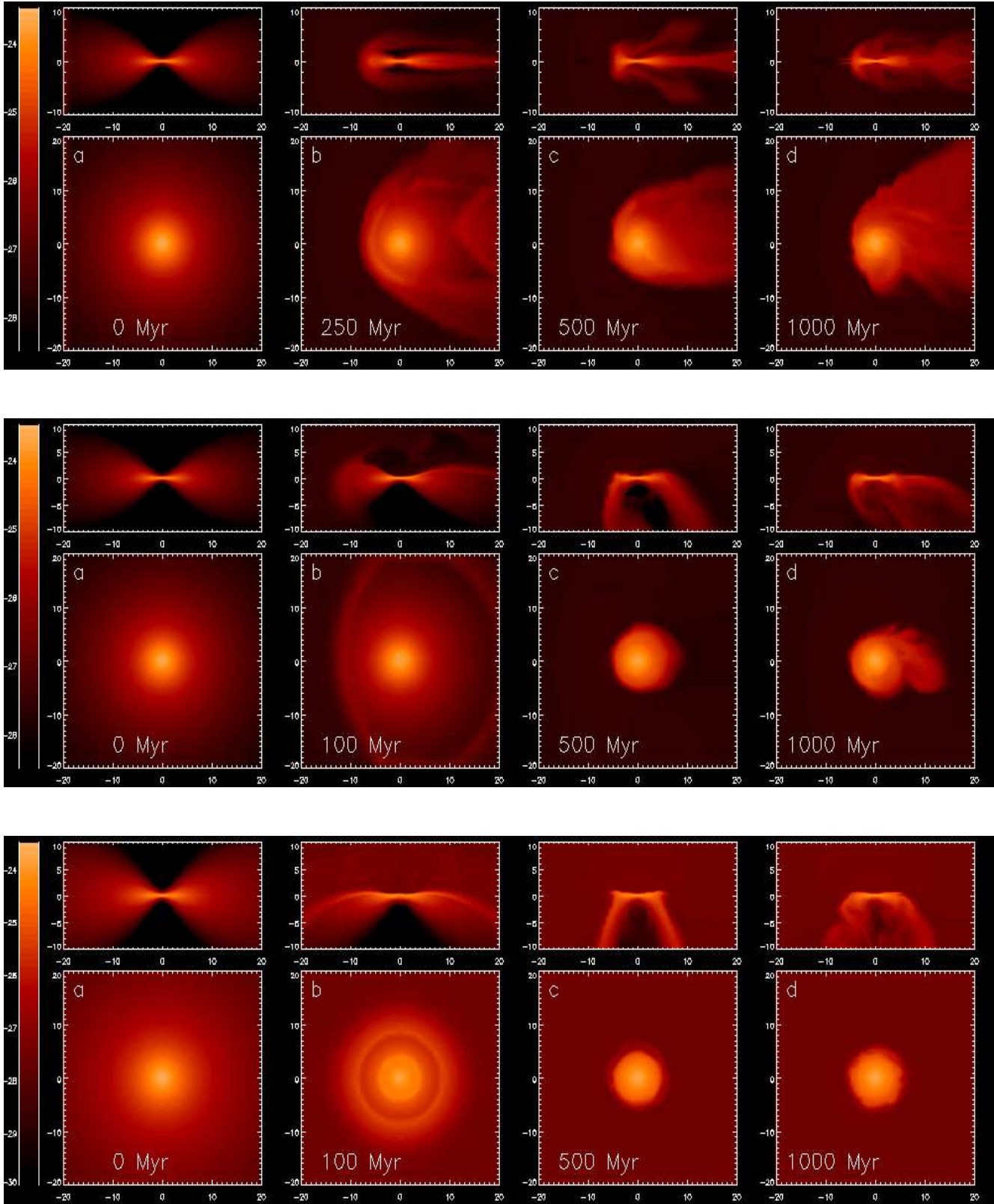


Figure 4. Evolution of the density for model MD-00-LO (upper strip), MD-45-LO (middle strip) and MD-90-LO (lower strip). In each strip the lower panels show the density map in the $z = 0$ plane, the upper panels show the density map in the $y = 0$ plane. Axes units are kpc.

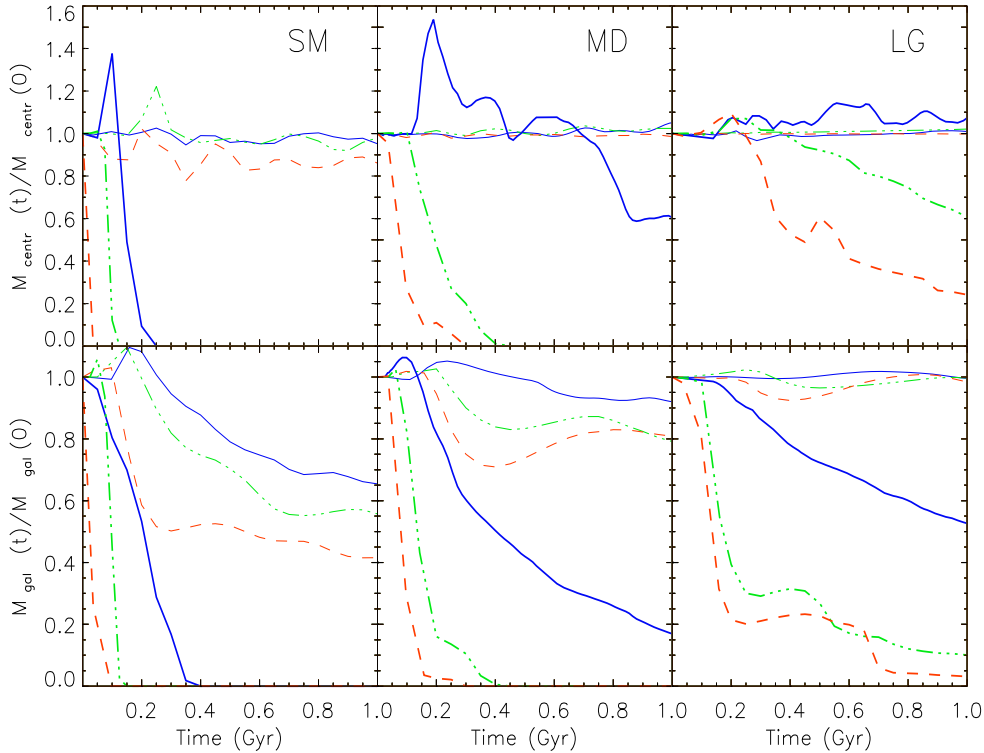


Figure 5. Evolution of the ISM mass in the “central region” (upper panels) and in the “galactic region” (lower panels). The mass refers to the cold gas with temperature $T < 3 \times 10^5$ K. From left to right the couples of lower and upper panels refer to SM, MD and LG. Solid blue lines: edge-on models; dashed-dotted green lines: 45° models; dashed red lines: face-on models. Light and heavy lines refer to LO and HI ram pressure models, respectively.

In Fig. 5 it is evident that, for the models MD-90-HI and MD-45-HI, the gas is completely removed from both the galactic and central regions after $\sim 2 - 4 \times 10^8$ yr. The edge-on model, instead, is more resistant to the stripping and retains more than 60% of its initial ISM in the central region after $t = 1$ Gyr. The gas amount in the whole galaxy has been reduced to $\sim 20\%$ of the initial value. This result appears contrary to the simple theoretical expectation of complete gas removal given by Fig. 3. However, $\tau_{\text{str}} > 1$ Gyr and M_{gal} is indeed still decreasing at $t = 1$ Gyr, as it is clear from Fig. 5. We verified that all the gas is removed from the galaxy after $t \sim 1.7$ Gyr.

As can be seen in Fig. 5, M_{centr} increases up to a maximum at 200 Myr for model MD-00-HI, and oscillates before decreasing by a factor of ~ 2 . At this point the radius of the galaxy has been reduced to $R_{\text{gal}} \sim 3$ kpc. The first maximum is related to the passage of the transmitted shock through the galaxy, while the oscillations reflect fluctuations of the ISM on the characteristic time scale ($\sim 2 \times 10^8$ Myr) of the sound crossing time of the central region. The magnitude of such oscillations strongly depends on our definition of central region; on larger scales the mass stripping proceeds in a more uniform fashion, as shown by the smooth behaviour of M_{gal} .

Given the different geometry of the IGM impact, the $\theta = 45^\circ$ and face-on models are more exposed to the effect of the ram pressure, and the stripping is complete after $t \sim 3 - 4 \times 10^8$ yr (Fig. 5).

5.2 Other models

5.2.1 Models SM

Now we examine the case of the smaller galaxy. Because of its shallower potential, it is the most sensitive to the influence of the IGM. From Fig. 3 we expect that the ISM evolution is not strongly dependent on the inclination angle.

The simulations broadly confirm this expectation. For model SM-LO, the central region is basically unaffected by the ram pressure for every θ . On the larger scale, M_{gal} rapidly decreases by a factor of ~ 2 in the face-on case because of the instantaneous stripping. After $t \sim 300$ Myr the stripping rate greatly reduces and M_{gal} decreases very slowly. The edge-on model, instead, loses mass at a lower and more uniform rate. This is because the continuous stripping is more effective than the instantaneous stripping, as expected given this specific geometry. Again, M_{centr} is essentially unaffected being $P_0 > P_{\text{ram}}$. At the end of the simulation the galactic radius is ~ 2 kpc and the ISM has a quite compact aspect.

In the model with stronger ram pressure (SM-HI), instead, the ISM is completely removed from the central region in few 10^8 yr and leaves the galaxy in $3 - 4 \times 10^8$ yr for any inclination. This is what we exactly expect from the theoretical analysis, so this kind of galaxy would show only its stellar component with no or very little gas content (see section 6). For model SM-00-HI the gas in the galactic region

temporary increases before to drop rather quickly. The density increase is due to the same mechanism discussed in the previous section for model MD-00-HI.

5.2.2 Models LG

This galaxy with its stronger gravitational field and central density is, of course, the least affected by ram pressure stripping. For the models with lower ram pressure (LG-LO) the stripping is minimal (see Fig. 5). In both regions under analysis the ISM mass does not vary significantly, for all values of θ . The final radius is quite large (> 20 kpc) and this galaxy is rather unperturbed also at large radii.

Even the higher ram pressure in models LG-HI is lower than (but close to) the central ISM pressure, $P_{\text{ram}}/P_0 \sim 0.66$. As discussed above, we expect that for $P_{\text{ram}} \sim P_0$ the inclination angle of the galaxy plays a crucial role. Indeed, as shown in Fig. 5, in the edge-on case M_{centr} is essentially unaffected by the ram pressure, while it decreases for the $\theta = 45^\circ$ model and even more for the face-on model. M_{gal} shows a behaviour similar to that of model SM-LO. In the edge-on case the mass loss is rather steady, while for models LG-45-HI and LG-90-HI the action of both the instantaneous and continuous stripping are apparent.

5.2.3 Models NR

We describe here the evolution of the ISM in a non rotating galaxy. As discussed in section 2.2, we are particularly interested to the fate of the ISM located at large radii. A spheroidal, extended gaseous halo could suffocate the galactic winds triggered by a central starburst, with important consequences for the chemical evolution of the galaxy. The ISM in this model, which has the same gravitational potential of model MD, but a higher ISM temperature (see section 2.3), extends initially to $R_{\text{ISM}} \sim z_{\text{ISM}} \sim 4$ kpc. The gas density distribution is rather flat near the galactic plane because of the influence of the stellar disc gravity, and becomes nearly spherical for $R, z \gtrsim 2$ kpc. The initial ISM surface density peaks at the center, $\Sigma(0) \sim 11 M_\odot \text{pc}^{-2}$, and drops rapidly with $R, \Sigma \sim 1.4 M_\odot \text{pc}^{-2}$ at $R \sim 1$ kpc and $\Sigma \sim 0.05 M_\odot \text{pc}^{-2}$ at $R \sim 2$ kpc. The central and galactic regions for this models are defined as two spherical volumes defined by $r \leq 1$ and $r \leq 4$ kpc respectively. The initial gas masses in these regions are $M_{\text{centr}} = 1.3 \times 10^7 M_\odot$ and $M_{\text{gal}} = 1.7 \times 10^7 M_\odot$ respectively. We report here only on face-on NR models (NR-LO and NR-HI). More non rotating galaxies will be discussed elsewhere (Marcolini et al. in preparation).

Model NR-LO loses gas at a nearly constant rate $\dot{M}_{\text{gal}} \sim 2.1 \times 10^6 M_\odot \text{Gyr}^{-1}$ and $\dot{M}_{\text{centr}} \sim 1.1 \times 10^6 M_\odot \text{Gyr}^{-1}$. For pedagogical reasons we run this model for a very long time $t = 10$ Gyr. The continuous ablation of the outer gas layers is the main process at work in this model, as expected being $P_0 > P_{\text{ram}}$. At $t \sim 300$ Myr the gas at large radii has been already stripped away and the ISM has a compact aspect. At this time, the ISM extends to a radius $R \sim 1.4$ kpc on the equatorial plane $z = 0$. Hereafter the stripping slowly reduces the size of the ISM which is completely removed in $t \sim 10$ Gyr (interestingly, being $P_0 > P_{\text{ram}}$, an incomplete stripping is expected according to the simple theory discussed in section 3). For most of the time the ISM distribution is asymmetric with respect to the $z = 0$ plane,

extending to $z \sim 0.5$ kpc upstream and to $z \sim -1 \div -1.8$ kpc in the cometary tail, depending on the time considered. We conclude that extended, spheroidal gaseous halos are unlikely to survive under the effect of (moderate) ram pressure stripping.

A backflow is generally present in this model, but it scarcely influences our results. Balsara, Livio and O'Dea 1994, Stevens, Acreman and Ponman 1999, Mori & Burkert 2000, among others, studied this backflow in some detail. In their calculations the accretion inflow occurs quasi-periodically, producing an oscillation in the rate of gas stripping. The accretion inflow disappears when the gas is not allowed to cool in the models of Balsara, Livio and O'Dea (1994), but it is instead present in the simulations of Mori & Burkert (2000) who neglect radiative losses. As discussed in section 6, the parameters of our models imply a general unimportance of the accretion backflow, independently on the effect of the radiative cooling.

In model NR-HI all the ISM is removed in ~ 500 Myr, as expected from the relation $P_0 < P_{\text{ram}}$. This time is in reasonable agreement with the timescale τ_{str} given by equation (12), $\tau_{\text{str}} \sim 400$ Myr, with $\dot{M} \sim \pi R_{\text{gal}}^2 \rho_{\text{IGM}} v_{\text{IGM}} \approx 2.5 \times 10^{23} \text{g s}^{-1}$, using an average $R_{\text{gal}} \sim 1$ kpc.

6 DISCUSSION AND CONCLUSIONS

We run several 3D and 2D hydrodynamic simulations of ram pressure stripping in galaxies moving through an external medium. We focused on the poorly investigated problem of disk dwarf galaxies located in small groups, where they are in fact more frequently observed. The ram pressures considered, $P_{\text{ram}} = 8 \times 10^{-14} - 3.2 \times 10^{-12} \text{dyn cm}^{-2}$ are one or two orders of magnitude lower than that expected in rich clusters, the subject of most previous studies. We run a set of models varying galactic mass (together with the relative size and gas content), inclination angle θ between galactic plane and orbital plane, and ram pressure strength.

Following Gunn & Gott (1972), we made simple analytic previsions of the disk radius beyond which the ISM is completely stripped in face-on models (section 3). We also extended the condition for ram pressure stripping to the edge-on models. Compared to the analytic estimates, the radii of our edge-on models tend to be a little larger after 1 Gyr. We can consider the time-scale τ_{str} given in equation (12) a rough estimate of the time needed by the ram pressure to ablate the galaxy to its final radius. In our models τ_{str} may be as long as a few Gyr, as confirmed by our numerical simulations. In fact, in some model the stripping is still going on at $t = 1$ Gyr, and thus the final radius is not yet reached at the end of the run. Given the simple assumptions on which the analytical model is based, the agreement with the numerical simulations is quite satisfactory.

We find that the inclination angle often plays a minor role. For $P_{\text{ram}} > P_0$ the galaxy is stripped for any inclination. In the case of $P_{\text{ram}} < P_0$ the amount of mass lost is rather independent of θ , with the edge-on models showing a slight tendency to retain more ISM (see Fig. 5). Only for $P_{\text{ram}} \sim P_0$ the ability of the galaxy to retain its ISM is significantly larger for $\theta = 0^\circ$. From the analysis presented in section 3 the final ISM radius R_{str} is expected to be more sensitive to θ for larger galaxies, as it is apparent

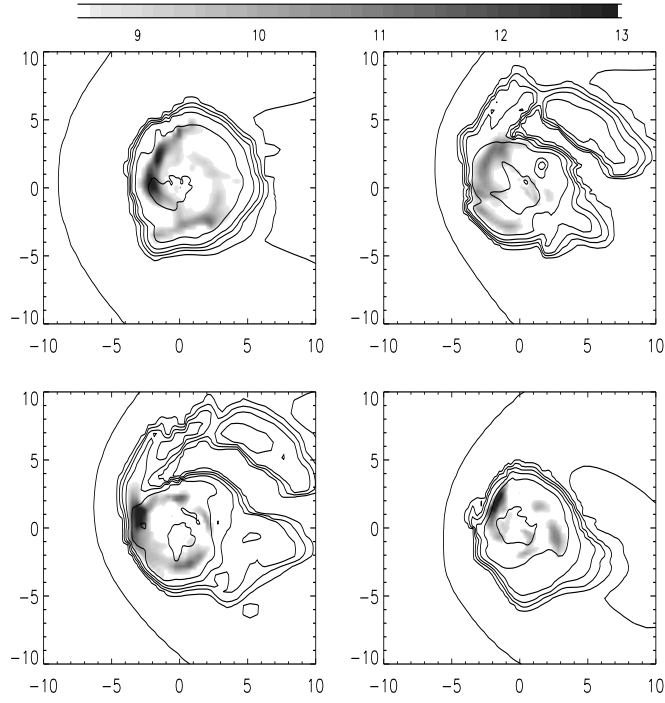


Figure 6. ISM face-on column density maps for model LG-45-HI. Only values larger than the critical value $\Sigma_g = 9M_\odot \text{pc}^{-2}$ are displayed. The time sequence is $t = (250, 350, 400, 550)$ Myr starting from the left-top panel and moving clockwise. The grey scale indicates Σ in units of $M_\odot \text{pc}^{-2}$. Contours represent the logarithm of ISM density on the galactic plane $z = 0$. The contour values are -26.5, -26.0, -25.5, -25.0, -24.5, -24.0 and -23.5. Axes units are kpc.

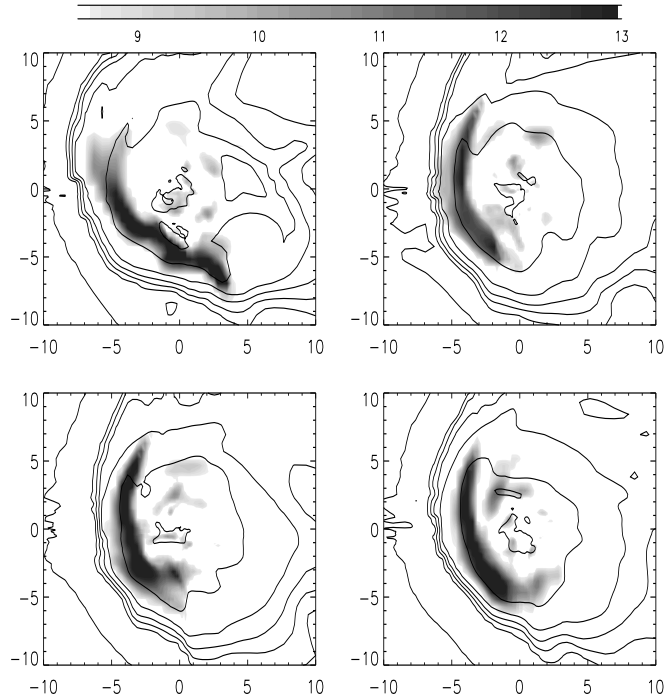


Figure 7. Same as Fig. 6 for model LG-00-HI. The various panels refer to $t = (380, 470, 510, 560)$ Myr. The contour values for the gas density are again -26.5, -26.0, -25.5, -25.0, -24.5, -24.0 and -23.5.

comparing the continuous curves (face-on galaxies) to their correspondent dashed curves in Fig. 3: only for the most massive galaxy the two curves differ significantly. The numerical simulations, however, show a stronger dependency of the effectiveness of the stripping on θ (and time). For both models MD and LG the mass of gas retained by the galaxy is indeed a sensitive function of θ for the stronger ram pressure (Fig. 5).

We note that when $P_{\text{ram}} < P_0$, the ISM can still be completely stripped, as discussed in section 5.2.3 for a non-rotating, nearly spherical galaxy (model NR-L0). However, in this case the time scale for the complete gas removal is very long, ~ 10 Gyr. This may imply that ancient dwarf galaxies in old poor groups, where the ram pressure is weak, may have their ISM removed. We note that the galaxy population in X-ray bright groups is indeed dominated by early-type (gas poor) dwarfs (e.g. Tran et al. 2001).

There is some debate in literature on the successors of stripped dwarf irregular galaxies. Conselice, Gallagher, & Wyse (2001) argue that dwarf elliptical galaxies presently seen in the core of the Virgo cluster cannot originate from field dwarfs accreted by the cluster. If this would be the case, very few post-stripped dwarf irregulars would be present in Virgo (Lee, McCall, & Richer 2003). However, other lines of evidence indicate that ram pressure stripping could have prevented many dIrrs in the present-day dEs (Lee, McCall, & Richer 2003; Conselice et al. 2003). In this scenario, tidal interactions with massive galaxies may provide the tool to transform rotationally supported stellar disks in slowly rotating, spheroidal galaxies (Mayer et al. 2001).

As discussed in section 5.2.3, several authors report the occurrence of an accretion inflow into the galactic core from the downstream side due to the gravitational force (Balsara, Livio and O’Dea 1994, Stevens, Acreman and Ponman 1999, Mori & Burkert 2000). This flow influences the stripping rate and may cause the appearance of a second bow shock (Balsara et al. 1994). We do not find any of the complexities described above in our rotating models. This is due to physical reasons and cannot be ascribed to the lower spatial resolution of our 3D simulations compared to the resolution of the 2D models described in the aforementioned papers. In fact, the behaviour of flows past gravitating bodies is in many cases determined by the ratio $\xi = \frac{2GM}{R(v^2+c^2)}$ (Balsara et al. 1994), where M and R are the mass and the radius of the gravitating body, v is the relative velocity and c the sound speed. In our models $\xi < 1$, and thus accretion is not supposed to occur. A (variable) backflow is present in some models, especially in model NR, but it does not accrete onto the galaxy and it does not influence the stripping rate

The efficiency of star formation is a strong function of the ISM pressure (Elmergreen & Efremov 1997). As the transmitted shock propagates through the galaxy, it may promote the collapse of molecular clouds inducing star formation. Obviously, we can not follow this phenomenon in our one-phase ISM models (see below). However, from the temporary increase of the ISM content in the galactic region of some models (see Fig. 5), we suspect that favourable conditions for star formation are possibly achieved in galaxies undergoing ram pressure stripping. More accurate considerations may be done taking into account the evolution of the ISM surface density Σ_{ISM} on the galactic plane of our models. Actually, episodes of star formation are believed to take

place in regions where the ISM surface density exceeds the critical value $\Sigma_{\text{cr}} \sim 9 M_{\odot} \text{pc}^{-2}$ (Gallagher & Hunter 1984; Skillman 1987, 1996), although this is not a sufficient condition (Dohm-Palmer et al. 2002). As an example, Fig. 6 shows maps of Σ_{ISM} on the galactic plane of the model LG-45-HI at several times. Σ_{ISM} is computed integrating in the interval $-z_{\text{centr}} < z < z_{\text{centr}}$ to neglect spurious contributions from clouds of gas located at larger $|z|$. Only values $\Sigma_{\text{ISM}} > \Sigma_{\text{cr}}$ are shown in Fig. 6, indicating regions where star formation is likely to occur. These regions are distributed rather stochastically both in space and time on a time span of 600 Myr. A stochastic pattern of star-forming regions is what Dohm-Palmer et al. (2002) find in the dwarf galaxy Sextans A. Of course, other external causes, such as tidal interactions with nearby galaxies, may also be responsible of star formation episodes. Moreover, in our models the largest supercritical values of Σ_{ISM} never occur in the galactic centre, where instead strong star burst are observed. We showed, however, that the IGM ram pressure in small groups may create the conditions for moderate and long lasting star formation in dwarf galaxies.

In general, the surface density increases more easily for small values of θ because a part of the gas is pushed to smaller galactic radii in the beginning of the stripping. This effect is also found by Vollmer et al. (2001), and Hidaka & Sofue (2002) find an increment of the molecular gas fraction in the central region of spiral galaxies suffering mild stripping. Possible episodes of star formation are expected to be triggered in this cases. In fact, our models LG-00-HI and MD-00-HI, which temporary increase their galactic gas content (Fig. 5), also present regions of supercritical surface density (Fig. 7). However, no direct link exists between mass content increase and surface density increase. In fact the model SM-00-HI, which also shows a “spike” in its galactic ISM content, never reaches a gas surface density larger than Σ_{cr} , and is completely stripped without any previous episode of star formation. On the contrary, in the models MD-45-HI and LG-45-HI, which never increase their galactic gas content, Σ_{g} episodically exceeds the critical value close to the galactic centre. Finally, the lowest value of ram pressure (LO) can not compress the ISM enough to obtain $\Sigma_{\text{g}} > \Sigma_{\text{cr}}$ for any value of θ and of galactic mass. From the above discussion we conclude that star bursts in dIrrs can be triggered by ram pressure in poor groups, but the galaxy must cross the group core, where larger values of P_{ram} occur.

All the above conclusions are obtained in the assumption that the ISM is distributed in a smooth fashion. Actually real ISM is a complex gaseous medium in which HI and massive molecular clouds are present. HI clouds have relatively low densities ($\sim 1 \text{cm}^{-3}$) and large sizes (~ 0.5 kpc) and readily react to external perturbations given by P_{ram} . We thus expect that their cumulative behaviour can be correctly described in the frame of single-phase ISM distribution. As pointed out above, we neglect the presence of molecular clouds because they are too small to be resolved by our simulations. In any case, given their large densities (100cm^{-3}) and small radii (~ 10 pc) they are much less affected by stripping processes (e.g. Raga et al. 1998). Differences in the response of HI and molecular clouds to ram pressure are found by Sofue (1994a,b).

In a successive paper we will consider the effect of a star

burst on the chemical and dynamical evolution of the ISM of dwarf galaxies undergoing ram pressure stripping.

ACKNOWLEDGEMENTS

We are grateful to the referee for his/her helpful suggestions which improved the presentation of the paper. We acknowledge financial support from National Institute for Astrophysics (INAF). The simulations were run at the CINECA Supercomputing Centre with CPU time provided by a grant of the National Institute for Astrophysics (INAF).

REFERENCES

- Abadi M.G., Moore B., & Bower R.G. 1999, MNRAS, 308, 947
 Balsara D., Livio M., & O’Dea C.P. 1994, ApJ, 437, 83
 Batchelor G.K. 1967, *An Introduction to Fluid Dynamics*, Cambridge University Press
 Bedogni R., & D’Ercole A. 1986, A&A, 157, 101
 Binney J., & Tremaine S. 1987, *Galactic Dynamics*. Princeton Univ. Press, Princeton
 Bureau M., & Carignan C. 2002, AJ, 123, 1316
 Conselice C.J., Gallagher J.S.III, & Wyse R.F.G., 2001, ApJ, 559, 791
 Conselice C.J., O’Neil K., Gallagher J.S.III, & Wyse R.F.G., 2003, submitted (astro-ph/0303185)
 De Young D.S. & Heckman T.M. 1994, ApJ, 431, 598
 D’Ercole A., & Brighenti F. 1999, MNRAS, 309, 941
 Dohm-Palmer R.C., Skillman E.D., Mateo M., Saha A., Dolphin A., Tolstoy E., Gallaher J.S., & Cole A.A. 2002, AJ, 123, 813
 Elmegreen B.G., & Efremov Y.N. 1997, ApJ, 480, 235
 Gallagher J.S., & Hunter D.A. 1984, ARA&A, 22, 37
 Grebel E.K., Gallaher J.S., & Harbeck D. 2003, astro-ph/0301025
 Gunn J., & Gott J. 1972, ApJ, 176, 1
 Heldson S.F. & Ponman T.J. 2000, MNRAS, 315, 356
 Hidaka M., & Sofue Y. 2002, PASJ, 54, 33
 Lee H., Mc Call M.L., & Richer M.G., 2003, submitted (astro-ph/0303359)
 Mac Low M.-M., & Ferrara A. 1999, ApJ, 513, 142
 Marcolini A. 2002, Tesi di Laurea, Bologna University
 Matteucci F., & Chiosi C. 1983, 1983, A&A, 123, 121
 Mayer L., Governato F., Colpi M., Moore B, Quinn T., et al., 2001, ApJ, 559, 754
 McKee C.F. 1988, in Roger R.S. & Landecker T.L. eds., *Supernova Remnants and the Interstellar Medium*, IAU Colloquium 101, Cambridge University Press, Cambridge, p. 205
 Mori M. & Burkert A. 2000, ApJ, 538, 559
 Murakami I. & Babul A. 1999, MNRAS, 309, 161
 Murray S.D., White S.D.M., Blondin J.M., & Lin D.N.C. 1993, ApJ, 407, 588
 Mushotzky R., Figueroa-Feliciano E., Lowenstein M., & Snowden S.L. 2003, astro-ph/0302267
 Nolthenius R. 1993, ApJS, 85, 1
 Norman M.L., Wilson J.R., & Burton R.T. 1980, ApJ, 239, 968
 Nulsen P.E.J. 1982, MNRAS, 198, 1007
 Quilis V., Moore B, & Bower R. 2000, *Science*, 288, 1617
 Raga A.C., Cantó J., Curiel S., & Taylor S. 1998, MNRAS, 295, 738
 Schulz S., & Struck C. 2001, MNRAS, 328, 185
 Skillman E.D. 1987, in Lonsdale Persson C.J., ed., NASA publ. CP2466, *Star Formation in Galaxies*, NASA, p. 263
 Skillman E.D. 1996, in Skillman E.D., ed., ASP Conf. Ser. Vol. 106, *The Minnesota Lectures on Extragalactic Neutral Hydrogen*. ASP, San Francisco, p. 208.
 Skillman E.D. 2001, ApSS (Suppl.), 277, 383
 Silich S., & Tenorio-Tagle G. 2001, ApJ, 552, 91
 Sofue Y., 1994a, ApJ, 423, 207
 Sofue Y., 1994b, PASJ, 46, 431
 Spitzer L. Jr. 1962, *Physics of Fully Ionized Gases*, Wiley (Interscience), New York
 Stevens I.R., Acreman D.M., & Ponman T.J. 1999, MNRAS, 310, 663
 Stone J.M. & Norman M.L. 1992, ApJS, 80, 753
 Strickland D.K., & Stevens I.R. 2000, MNRAS, 314, 511
 Swaters R.A. 1999, Ph. D thesis, Rijksuniversiteit Groningen
 Tassoul J-L. 1978, *Theory of Rotating Stars*, Princeton University Press
 Tenorio-Tagle G. 1996, AJ, 111, 1641
 Tran K-V.H., Simard L., Zabludoff A.I., Mulchaey J.S., 2001, ApJ, 549, 172
 Van den Bergh S. 1994, ApJ, 428, 617
 Vollmer B., Cayatte V., Balkowski C., & Duschl W.J. 2001, ApJ, 561, 708
 Zabludoff A.I., & Mulchaey J.S. 1998, ApJ, 496, 39